Journal of Luminescence 130 (2010) 728–732

Contents lists available at ScienceDirect

Journal of Luminescence

journal homepage: www.elsevier.com/locate/jlumin

Heat-treatment-induced luminescence degradation in Tb^{3+}-doped $CePO_4$ nanorods

Weihua Di *, Xiaoxia Zhao, Zhaogang Nie, Xiaojun Wang, Shaozhe Lu, Haifeng Zhao, Xinguang Ren

Key Laboratory of Excited State Processes, Changchun Institute of Optics, Fine Mechanics and Physics, Chinese Academic of Sciences, 16 Eastern Nanhu Road, Changhcun 130033, PR China

ARTICLE INFO

Article history:
Received 10 January 2007
Received in revised form
17 November 2009
Accepted 30 November 2009
Available online 6 December 2009

Keywords:
Ce^{3+}
Tb^{3+}
Ce^{4+}
Photoluminescence
Thermal degradation

ABSTRACT

$CePO_4$:Tb nanorods were synthesized via a simple wet-chemical route. The as-synthesized $CePO_4$:Tb nanorods present high photoluminescence efficiency due to an efficient energy transfer form Ce^{3+} to Tb^{3+}. However, heat treatment at 150 °C in air leads to a significant decrease of photoluminescence. X-ray photoelectron spectroscopy and excitation spectra revealed the oxidation of Ce^{3+} to Ce^{4+} in the heat-treatment process, which should be responsible for significant photoluminescence degradation due to the breakage of $Ce^{3+} \rightarrow Tb^{3+}$ energy transfer. This conclusion is further supported by atmosphere and size effects of photoluminescence of $CePO_4$:Tb under the heat treatment.

1. Introduction

Nowadays, inorganic luminescent materials with nanometer dimensions have become an important field of modern nanoscale science and technology, which could find numerous potential applications in the fields of physics, chemistry and biology [1,2]. In particular, one-dimensional (1D) luminescent nanostructures have attracted considerable attention due to their potential as interconnectors and active components in fabricating optoelectronic devices [3,4].

Rare earth compounds have been widely used in high-performance luminescent devices, magnets, catalysts and other functional materials owing to numerous well-defined transition modes involving the 4f shell of their ions [5]. Recently, more and more interest has been focused on the synthesis and photoluminescence of rare earth orthophosphates of nanosize scale for their potential application in optoelectronic devices and biological fluorescence labeling [6,7].

It is well known that Ce^{3+}- and Tb^{3+}-doped materials (e.g., $LaPO_4$:Ce,Tb; $CePO_4$:Tb) are efficient green-emitting phosphors due to high efficiency of energy transfer from Ce^{3+} to Tb^{3+}[8,9], and they are extensively applied in fluorescent lamps (FLs), cathode ray tubes (CRTs) and plasma display panels (PDPs) as green-emitting components [10,11]. Riwotzki et al. [12] reported the synthesis and photoluminescence characteristic of $CePO_4$:Tb colloidal nanocrystals . Kompe et al. [13] reported the luminescence enhancement in $CePO_4$:Tb@$LaPO_4$ core–shell structures. Yu et al. [14] investigated the difference in photoluminescence properties between $LaPO_4$:Ce,Tb nanorods and nanowires. However, investigations about thermal stability of Ce- and Tb-doped nanophosphors have not been reported up to now based on our present knowledge.

As a matter of fact, heat treatment in air is a necessary procedure in the manufacturing of optoelectronic devices [15]. Ce^{3+} ions are well known to be highly temperature-sensitive since they are oxidized to Ce^{4+} ions easily [16]. Therefore, from a practical point of view, an investigation on the effect of heat treatments on photoluminescence properties of Ce^{3+}- and Tb^{3+}-doped nanophosphors is of great significance. For this reason, this work aims at reporting the heat-treatment effect of photoluminescence of Tb^{3+}-doped $CePO_4$ nanorods, as well as the thermal degradation mechanism.

2. Experimental

$Ce_{0.95}PO_4$:$Tb_{0.05}$ nanorods were synthesized via a simple wet-chemical route as follows. Typically, appropriate amounts of high purity Tb_4O_7 were dissolved in concentrated HNO_3 to form $Tb(NO_3)_3 \cdot 6H_2O$. Appropriate quantities of $Tb(NO_3)_3 \cdot 6H_2O$ and $CeCl_3 \cdot 7H_2O$ were dissolved in deionized water; 10 mL of $(NH_4)_2HPO_4$ solution (0.1 M) was added slowly to 20 mL of the mixed solution of $CeCl_3$ (0.0475 M) and $Tb(NO_3)_3$ (0.0025 M). The

* Corresponding author. Fax: +86 431 6176338.
E-mail address: weihdi@yahoo.com.cn (W. Di).

0022-2313/$ - see front matter © 2009 Elsevier B.V. All rights reserved.
doi:10.1016/j.jlumin.2009.11.034

final pH value was adjusted to 1–2 by addition of aqueous ammonia (NH_4OH). After good stirring for 1 h, the formed suspensions were poured into a Teflon-lined stainless steel autoclave and purged with argon for 60 min to prevent the oxidation of Ce^{3+} to Ce^{4+} before heating. The autoclave was sealed and maintained at 100 °C for 24 h, and then air-cooled down to room temperature. The resulting $CePO_4$:Tb products were washed and centrifuged. This process was repeated several times. The white precipitates were dried at 60 °C in vacuum.

Crystal structure and morphology of the samples were obtained by X-ray diffraction (XRD) using a Cu target radiation resource (λ=1.54078 Å) and scanning electron microscopy (SEM) using a Hitachi S-4800 scanning electron microscope, respectively. Fluorescence spectra were recorded with a Hitachi F-4500 fluorescence spectrometer at room temperature. In the measurement of the fluorescent decay of Tb^{3+}, 266-nm light generated from a fourth-harmonic generator pumped by a pulsed Nd:YAG laser was used as the excitation source. X-ray photoelectron spectroscopy (XPS) analysis was performed using a PHI Quantera SXM (ULVAC-PHI) device operating at a pressure of 10^{-8} Torr. The photoelectron emission spectra were recorded using a monochromatic AlKα source (100 W). The angle between the X-ray direction and the emitted electron direction was 45°.

3. Results and discussion

3.1. XRD, SEM and photoluminescence

Fig. 1 shows XRD pattern of the as-synthesized and heat-treated samples. It is noted that all the diffraction peaks could be well indexed to a hexagonal rhabdophane-type $CePO_4$ hydrate (JCPDS No. 35-0614). The broad diffraction peaks indicate small size of the as-synthesized products. For the sample thermally treated at 150 °C for 45 min, no additional phase was found during the thermal treatment. It can be seen from the SEM image (Fig. 2) that the as-synthesized sample exhibits rod-like morphology with a diameter of 20–30 nm and a length of 150–250 nm.

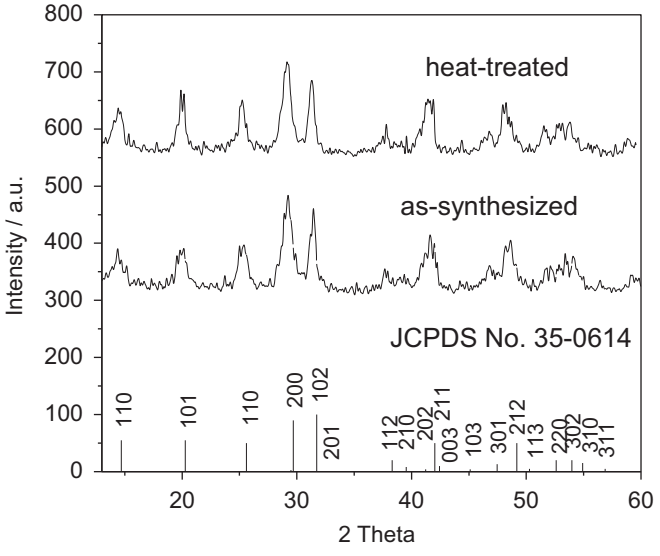

Fig. 1. XRD patterns of the as-synthesized $CePO_4$:Tb hydrate and that heat treated at 150 °C for 45 min in air. The standard XRD pattern of JCPDS File No. 35-0614 ($CePO_4$ hydrate) is also shown (bottom).

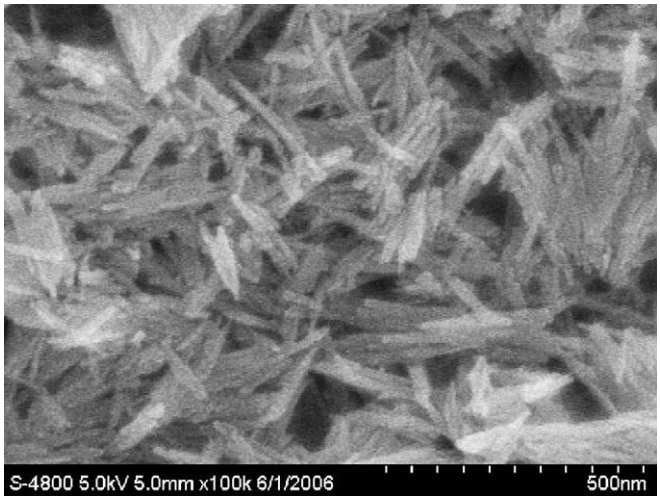

Fig. 2. SEM image of $CePO_4$:Tb hydrate.

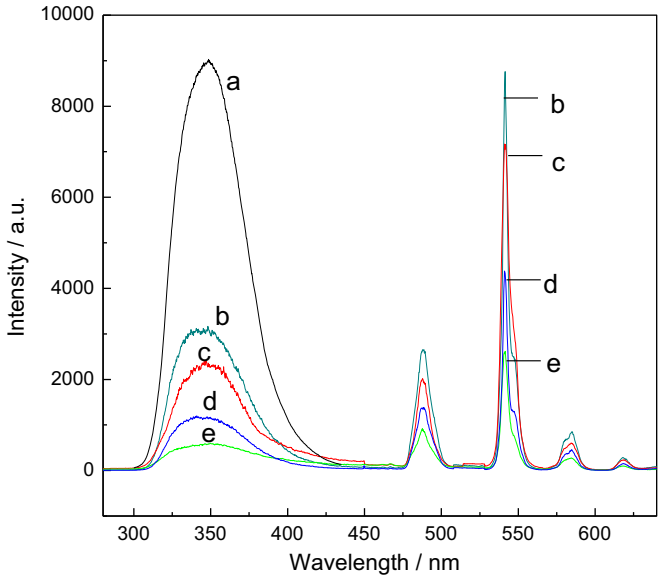

Fig. 3. Emission spectra of undoped $CePO_4$ —a and Tb-doped $CePO_4$, as-synthesized $CePO_4$:Tb—b and those heated at 150 °C for 15 min —c, for 30 min—d and for 45 min—e with 275-nm excitation.

Fig. 3 shows the emission spectra of $CePO_4$ and $CePO_4$:$Tb_{0.05}$ for 275-nm excitation. For undoped $CePO_4$, one can observe broad band emission of Ce^{3+} centered around 355 nm, which originates from transitions from the lowest component of the ^2D state to the spin–orbit components of the ground state, $^2F_{7/2}$ and $^2F_{5/2}$ [12]. When 5% Tb^{3+} was doped in the $CePO_4$ host, the emission of Ce^{3+} decreases significantly, whereas the characteristic emission of Tb^{3+} was observed, which originates from the transition between different f-electron states of Tb^{3+}, i.e., from the excited $^5D_4$ to the ground states ^7F_j (j=6, 5, 4, 3) [17]. This indicates efficient energy transfer from Ce^{3+} to Tb^{3+}. This energy transfer behavior is also evidenced by the excitation spectrum (Fig. 4) monitored within the $^5D_4$–$^7F_5$ emission of Tb^{3+}, in which the characteristic absorption of Ce^{3+} is observed due to the transitions from the ground state $^2F_{5/2}$ of Ce^{3+} to the different components of the excited 5d states split by the crystal field [12].

The emission decay curve of $^5D_4$–$^7F_5$ for Tb^{3+} is shown in Fig. 5. It can be seen that the emission decay of $^5D_4$ of Tb^{3+} in the as-synthesized sample deviates slightly from single-exponential

behavior, and can be well fitted by a bi-exponential function. This can be explained by the presence of structural water, which acts as nonradiative transition channels [4,17].

3.2. Thermal degradation of photoluminescence and its origin

It can be observed from Fig. 3 that the heat treatment in air leads to a decrease of the emission intensity of Ce^{3+}. With an increase of heat-treatment time, the decrease of emission intensity becomes more pronounced. Thermal degradation of Tb^{3+} luminescence is also observed, similar to that of Ce^{3+}.

To reveal the origin of luminescence degradation during the heat-treatment process, X-ray photoelectron spectroscopy (XPS) was used to determine the local atomic environment and chemical states of material surface. Fig. 6 presents the Ce3d XPS spectra of the original $CePO_4$:Tb nanrods and those samples heat

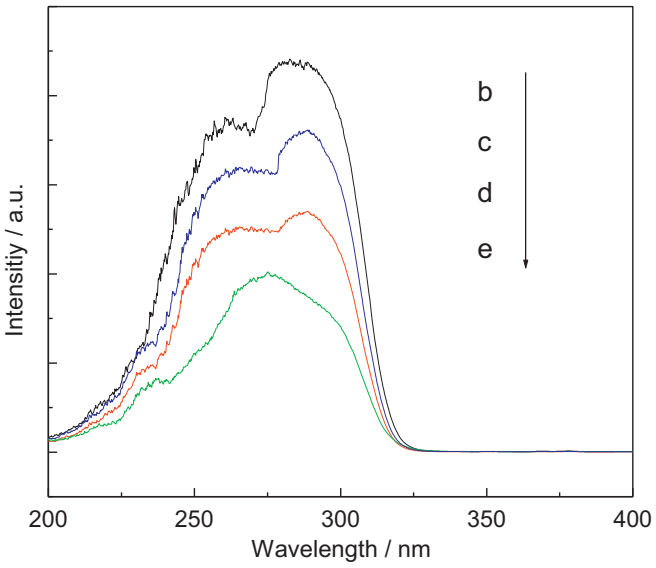

Fig. 4. Excitation spectra of as-synthesized $CePO_4$:Tb—b, and those heated at 150 °C for 15 min—c, for 30 min—d and for 45 min—e. The emission wavelength monitored is 545 nm.

treated under different atmospheres. For the original sample, the $Ce3d_{3/2,5/2}$ spectra are composed of two multilets (v and u) corresponding to the spin–orbit split $3d_{5/2}$ and $3d_{3/2}$ core holes, respectively. The four peaks resolved from this pair of spin–orbit doublets can be identified as those of the Ce^{3+} state: the higher binding energy peaks, u′ and v′, located at about 903.8 ± 0.1 eV and 885.4 ± 0.1 eV, respectively, are the result of $Ce3d^94f^1\ O2p^6$ final state, while the lower binding energy, u″ and v″, located at 900.8 ± 0.1 eV and 882 ± 0.1 eV, are the result of $Ce3d^94f^2\ O2p^5$ [18]. However, for the sample exposed to air at 150 °C for 45 min, an additional peak located at 916 eV is clearly observed. This peak is characteristic of Ce^{4+} state originating from $Ce3d^94f^0\ O2p^6$ final state [18]. This clearly demonstrates the presence of Ce^{4+} at the surface for the sample exposed to air at 150 °C.

As illustrated earlier, the strong luminescence of Tb^{3+}-doped $CePO_4$ is generated mainly through Ce^{3+} sensitization. Therefore, the presence of Ce^{4+} at the expense of Ce^{3+} reduces the emission of Ce^{3+} and its sensitization to Tb^{3+}. In the excitation spectra (Fig. 4), it can be seen that the absorption of Ce^{3+} is reduced significantly with the thermal treatment in air. This further provides evidence for the oxidation of Ce^{3+} to Ce^{4+}. The thermal oxidation Ce^{3+} to Ce^{4+} in air results in a decrease of the number of Ce^{3+}, and consequently, the excitation energy absorbed by Ce^{3+}, which is subsequently transferred to Tb^{3+}, is reduced. This is an apparent reason why the emission efficiency of $CePO_4$:Tb nanorods decreases during the thermal treatment process in air.

3.3. Atmosphere effect

To confirm the effect of thermal oxidation of Ce^{3+} on photoluminescence, the sample subjected to air at 150 °C was heat treated in a reducing atmosphere (H_2/Ar). The XPS result shows that when the sample subjected to thermal oxidation was exposed to the reducing atmosphere at 200 °C for 30 min, the signal indicative of Ce^{4+} state disappears totally, fully recovering to the initial Ce^{3+} state (Fig. 6c), demonstrating the reduction of the oxidized states of Ce. The emission intensity of Ce^{3+} and Tb^{3+} was recovered to the initial level. This means the oxidized states of Ce can be reversibly returned to Ce^{3+}, leading to the recovery of luminescence.

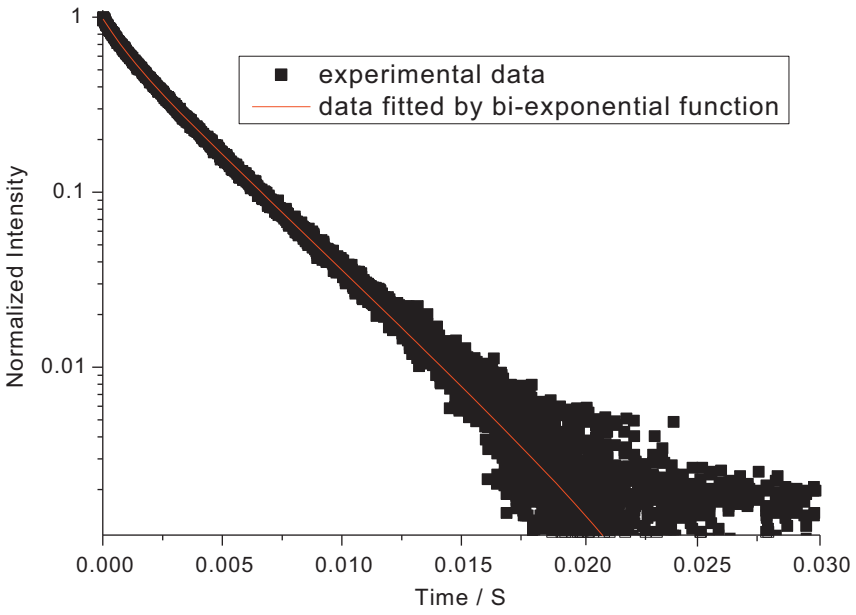

Fig. 5. Fluorescence decay curves of $^5D_4$ of Tb^{3+} in the as-synthesized $CePO_4$:Tb. The emission wavelength monitored is 545 nm.

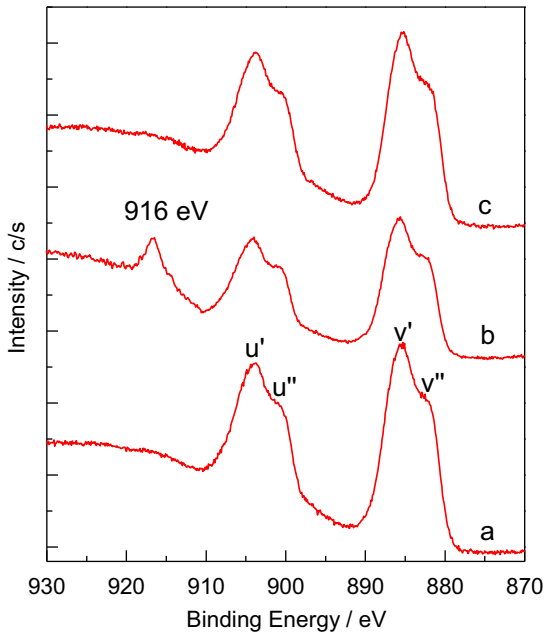

Fig. 6. XPS spectra recorded from Ce3d$_{3/2,5/2}$ for the original $CePO_4$:Tb —a, that exposed to air at 150°C for 45 min —b and then exposed to reducing gas (H_2/Ar) at 200 °C for 30 min—c.

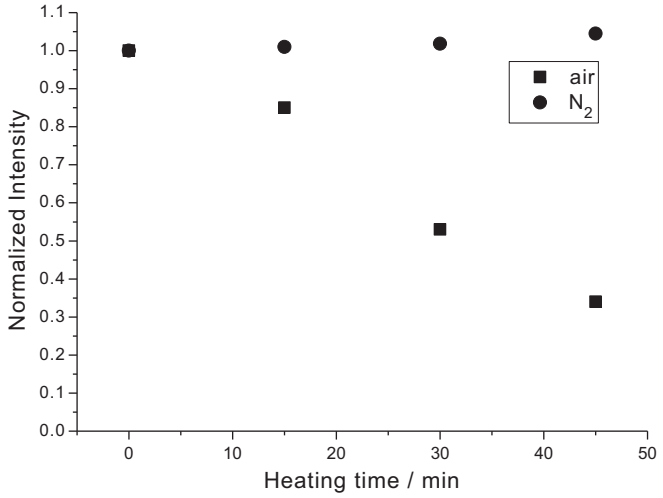

Fig. 7. Emission intensity of $CePO_4$:Tb as a function of time of heat treatment in air and N_2.

In order to further prove the effect of Ce^{3+} oxidation on luminescence properties, the as-synthesized sample was thermally treated in N_2 (protection atmosphere) for a comparison with the sample thermally treated in air. The emission intensity of the thermal-treated sample in air decreases rapidly with time of heat treatment, while that of heat-treated sample in N_2 shows a slight increase with time, as shown in Fig. 7. This further indicates that the thermal oxidation of Ce^{3+} to Ce^{4+} in air effectively reduces the luminescence efficiency of $CePO_4$:Tb nanorods.

3.4. Size effect

For a comparison, $CePO_4$:Tb bulk sample with the same composition as that of the nanorods was prepared using solid state reaction (SSR). The size of the particles prepared by SSR was about 1–2 μm. The result shows that the emission intensity of bulk samples has a decrease of only 5% with the heat treatment in air at 150 °C for 45 min. However, for $CePO_4$:Tb nanorods, the total emission intensity of Ce^{3+} and Tb^{3+} decreases to 35%. This indicates a strong thermal degradation effect of luminescence of $CePO_4$:Tb nanorods, which should be associated with the size of synthesized products. Due to a large surface-to-volume ratio for $CePO_4$:Tb nanorods with a diameter of 20–30 nm and a length of 150–250 nm, a large percentage of atoms are located at the surface [19,20]. As expected, there are a large number of Ce^{3+} ions located at the surface; as a result, a strong thermal oxidation effect occurs at the surface for small-sized samples, compared with the case of the bulk sample. In addition, low crystallinity and disordered environment around the surface of $CePO_4$:Tb nanorods also contributes to the oxidation of Ce^{3+} to Ce^{4+}. Therefore, improvement of the thermal stability for $CePO_4$:Tb nanomaterials is necessary, since their application in optoelectronic devices requires thermal treatment and this process significantly reduces the luminescence efficiency [15]. It is necessary to search for a suitable way to resist the thermal oxidation of Ce^{3+} in order to obtain efficient and stable $CePO_4$:Tb nanophosphors. One possible strategy is the formation of core–shell structure [20,21], because this shell might act as a protective layer against the thermal oxidation. The related research is ongoing.

4. Conclusions

Tb^{3+}-doped $CePO_4$ nanorods have been successfully synthesized by a hydrothermal route. A significant thermal degradation effect of photoluminescence for $CePO_4$:Tb nanorods was observed. The X-ray photoelectron spectroscopy and excitation spectra revealed that the oxidation of Ce^{3+} to Ce^{4+} in the heat treatment in air should be responsible for significant photoluminescence degradation due to breakage of the $Ce^{3+} \rightarrow Tb^{3+}$ energy transfer. The size effect of photoluminescence of $CePO_4$:Tb under the heat treatment demonstrated poor thermal stability of nanoscaled materials.

Acknowledgements

This work was partially supported by the National Natural Science Foundation of China (Grant no. 50502031) and Natural Science Foundation of Jilin Province(Grant no. 20060522). W. Di is grateful for the special starting research fund for the Awardees of President Prize of Chinese Academy of Sciences.

References

[1] T. Jüstel, H. Nikol, C. Ronda, Angew. Chem. Int. Ed. 41 (1998) 3084.
[2] G. Hebbink, J. Stouwdam, D. Reinhoudt, E. Beggel, Adv. Mater. 14 (2002) 1147.
[3] X. Duan, Y. Huang, Y. Cui, J. Wang, C. Lieber, Nature 409 (2001) 409.
[4] W.H. Di, X.J. Wang, P.F. Zhu, B.J. Chen, J. Solid State Chem. 180 (2007) 467.
[5] X. Wang, Y.D. Li, Chem. Eur. J. 9 (2003) 5627.
[6] W.H. Di, M.G. Willinger, R.A.S. Ferreira, X.G. Ren, S.Z. Lu, N. Pinna, J. Phys. Chem. C 112 (2008) 18815.
[7] F. Meiser, C. Cortez, F. Caruso, Angew. Chem., Int. Ed. 43 (2004) 5954.
[8] G. Blasse, B.C. grabmaierLuminescent Materials, Springer, Berlin, 1994.
[9] O.A. Serra, E.J. Nassar, G. Zapparolli, I.L.V. Rosa, J. Alloys Compd. 225 (1995) 63.
[10] J. Dexpert-Ghys, R. Mauricot, M.D. Faucher, J. Lumin. 69 (1996) 203.
[11] B. Monie, G. Bizarri, Mater. Sci. Eng. B 105 (2003) 2.
[12] K. Riwotzki, H. Meyssamy, H. Schnablegger, A. Kornowski, M. Haase, Angew. Chem. Int. Ed. 40 (2001) 573.
[13] K. Kompe, H. Borchert, J. Storz, A. Lobo, S. Adam, T. Moller, M. Haase, Angew. Chem. Int. Ed. 42 (2003) 5513.
[14] L.X. Yu, H.W. Song, Z.X. Liu, L.M. Yang, S.Z. Lu, Z.H. Zheng, J. Phys. Chem. B 109 (2005) 11450.
[15] K.S. Sohn, S.S. Kim, H.D. Park, Appl. Phys. Lett. 81 (2002) 1759.

[16] S. Deshpande, S. Patil, S.VNT. Kuchibhatla, S. SealAppl. Phys. Lett. 87 (2005) 133113.
[17] W.H. Di, X.J. Wang, B.J. Chen, S.Z. Lu, X.X. Zhao, J. Phys. Chem. B 109 (2005) 13154.
[18] Y. Takita, X. Qing, A. Takami, H. Nishiguchi, K. Nagaoka, Appl. Catal. A 296 (2005) 63.
[19] C.H. Yan, L.D. Sun, C.S. Liao, Y.X. Zhang, Y.Q. Lu, S.H. Huang, S.Z. Lu, Appl. Phys. Lett. 19 (2003) 3511.
[20] O. Lehmann, M. Karsten Kompe, J. Haase, Am. Chem. Soc. 126 (2004) 14935.
[21] W. Stouwdam, F.C.J.M. van Veggel, Langmuir 20 (2004) 11763.